

# THE PHYSICAL REVIEW

*A journal of experimental and theoretical physics established by E. L. Nichols in 1893*

SECOND SERIES, VOL. 71, No. 2

JANUARY 15, 1947

## Slow Neutron Velocity Spectrometer Studies I. Cd, Ag, Sb, Ir, Mn\*

L. J. RAINWATER, W. W. HAVENS, JR., C. S. WU, AND J. R. DUNNING  
*Columbia University, New York, New York*

(Received October 19, 1946)

The Columbia Neutron Velocity Spectrometer has been completely redesigned and enlarged to permit 32 separate measurements to be made simultaneously with greatly improved resolution and precision. A detailed comparison between the experimentally measured cross section of Cd and the Breit-Wigner one-level formula gives excellent agreement for over a factor of 100 in energy and 1000 in cross section. The selected parameters are  $\sigma_0 = (7200 \pm 200)$ ,  $E_0 = (0.176 \pm 0.002)$  ev, and  $\Gamma = (0.115 \pm 0.002)$  ev with a value of  $(5.3 \pm 0.7)$  added as a "constant" term in the total cross section. (Energy is in ev and cross sections in units of  $\times 10^{-24}$  cm<sup>2</sup>/atom.) The silver resonance levels have been remeasured with essential agreement with the previous results. Three levels are well defined at  $(5.1 \pm 0.1)$  ev,  $(16 \pm 1)$  ev, and  $(45 \pm 4)$  ev. Antimony has also been checked and the upper "level" has been partially resolved

into two levels at  $(15 \pm 1)$  ev and  $(21 \pm 1.5)$  ev. The other level is at  $(5.8 \pm 0.15)$  ev and there is no indication of higher energy levels. Manganese is found to have a strong level at  $(300 \pm 40)$  ev and probably other unresolved higher energy levels. There is no indication of levels at lower energies where the cross section shows a normal  $1/v$  type absorption with

$$\sigma = [(2.26 \pm 0.4) + (2.24 \pm 0.05)E^{-1/2}].$$

The iridium curve shows high detail. This includes strong levels at  $(0.64 \pm 0.015)$  ev,  $(1.27 \pm 0.04)$  ev,  $(5.2 \pm 0.2)$  ev, and  $(8.7 \pm 0.3)$  ev. There is a low broad transmission dip for energies above about 20 ev, indicating several more levels may be present. A  $1/v$ -type absorption is observed in the thermal region with  $\sigma = [(14 \pm 6) + (64 \pm 2)E^{-1/2}]$ . Further analysis has been made for most of the resonances.

### INTRODUCTION

#### Previous Measurements

IN two previous papers<sup>1,2</sup> a description has been given of a neutron spectrometer system developed for use with the Columbia University cyclotron. The factors involved in the use of such an instrument were discussed in detail and results

given for the slow neutron cross sections *vs.* energy for Cd, B, Li, Ag, In, Sb, Hg, and Au. Since the completion of the measurements described in these references, the spectrometer system has been redesigned to permit much improved operation. These improvements, to be discussed in more detail below, consist mainly of the following: (a) The number of timing intervals to be simultaneously measured was increased to 16 for each of two measuring channels. This permits 32 separate measurements to be made simultaneously. The resulting increase in efficiency makes practical operation with greater resolution and statistical accuracy and also increases the rate at which the measurements may be made. (b) The basic circuits were completely redesigned to have fractional microsecond re-

\* This document is based on work performed under Contract W-7405-Eng. 50 with the Manhattan Project at Columbia University. It will also appear in Book III, Division VIII, in the Manhattan Project Technical Series as part of the contribution of the Physics Department, Columbia University. Publication assisted by the Ernest Kempton Adams Fund for Physical Research of Columbia University, New York, New York.

<sup>1</sup>J. Rainwater and W. Havens, Phys. Rev. **70**, 136 (1946).

<sup>2</sup>W. Havens and J. Rainwater, Phys. Rev. **70**, 154 (1946).

sponse characteristics. This improves the resolution and precision of the system particularly for work at higher energies. (c) The timing is now accomplished automatically by setting 4 switches rather than by individual visual adjustment of all pulse widths. The resultant timings are as stable as the 100 Kc crystal oscillator which serves as the frequency standard. The use of successive "scale-of-2" and "chain" type scaling circuits permits precise control of all timing intervals. (d) The source detector path length has been increased to 6.2 meters and the  $\text{BF}_3$  proportional counter length decreased to 10 cm to improve the resolution. A thinner source slab decreases the thermal delay correction to about 30 microseconds. (e) Much improved shielding with thick paraffin, boron, and Cd at the source position and around the collimating tubes and detector have greatly decreased the background intensity for high energy measurements (over 10 ev).

Since the new system has been in operation a large number of elements have been investigated and the earlier measurements<sup>1,2</sup> have been rechecked. This paper is the first of a series of papers in which the results of these measurements will be presented.

#### CHOICE OF ELEMENTS FOR STUDY

##### Cadmium

In the first reference results were given of measurements of the slow neutron cross section of cadmium as a function of energy. It was shown that there was good quantitative agreement between the experimentally measured cross sections *vs.* energy and those predicted by the Breit-Wigner one-level formula

$$\sigma(E) = \frac{\sigma_0 \Gamma^2 (E_0/E)^{1/2}}{\Gamma^2 + 4(E - E_0)^2}.$$

Values of  $\sigma_0 = (7800 \pm 800) \times 10^{-24}$  cm<sup>2</sup>/atom,  $E_0 = (0.180 \pm 0.008)$  ev, and  $\Gamma = (0.112 \pm 0.006)$  ev were obtained for the cross section at exact resonance, the energy at exact resonance, and the half-width of the level. Since the Breit-Wigner one-level formula is widely used in connection with slow neutron capture theory, and since the cadmium resonance is almost unique in its suitability for detailed comparison with the theory, it was considered to be of interest to

repeat the cadmium measurements with better resolution and statistical accuracy and to extend the range of the measurements to higher energies to obtain a detailed comparison over the widest possible range of energies and cross sections. In the measurements to be described below comparison has been made for over 80 different values of the neutron energy between 0.0083 ev and 2.11 ev corresponding to a range of cross sections from 7200 to 6 ( $\times 10^{-24}$  cm<sup>2</sup>/atom). (The above values are not corrected for the fact that only one isotope of Cd is responsible for the resonance.)

##### Silver

In the earlier measurements for silver<sup>2</sup> precise results were obtained for the thermal cross sections including the "constant" term and the  $1/v$  slope of the cross section in the thermal region. The main resonance at  $(5.1 \pm 0.2)$  ev was also clearly shown and there was evidence of other levels at  $(13.7 \pm 2)$  ev and  $(43 \pm 5)$  ev. Since measurements are now easily made with better precision and resolution in the high energy region, these measurements were repeated. The new results (described below) are in substantial agreement with those of the earlier measurements.

##### Antimony

The previous measurements for antimony<sup>2</sup> showed that two levels were present near 6 ev and 19 ev with indication of a higher level or levels. The cross section in the thermal energy region was measured with some precision and the " $1/v$  factor slope" and the "constant" terms in the thermal cross section were determined. The high energy region has been reinvestigated with maximum resolution. The lower level at 5.8 ev remains single whereas the upper "level" splits into two almost equal levels at 15 and 21 ev. No evidence for resonances at still higher energies was found.

##### Manganese

Manganese is of considerable interest for slow neutron experiments because of its extensive use as a radioactive slow neutron detector. Previous attempts<sup>3-5</sup> to determine the energy of the Mn

<sup>3</sup> W. J. Horvath and E. O. Salant, Phys. Rev. **59**, 154 (1941).

<sup>4</sup> H. Feeny and F. Rasetti, Can. J. Research **23A**, 12 (1945).

<sup>5</sup> H. Goldsmith and F. Rasetti, Phys. Rev. **50**, 328 (1936).

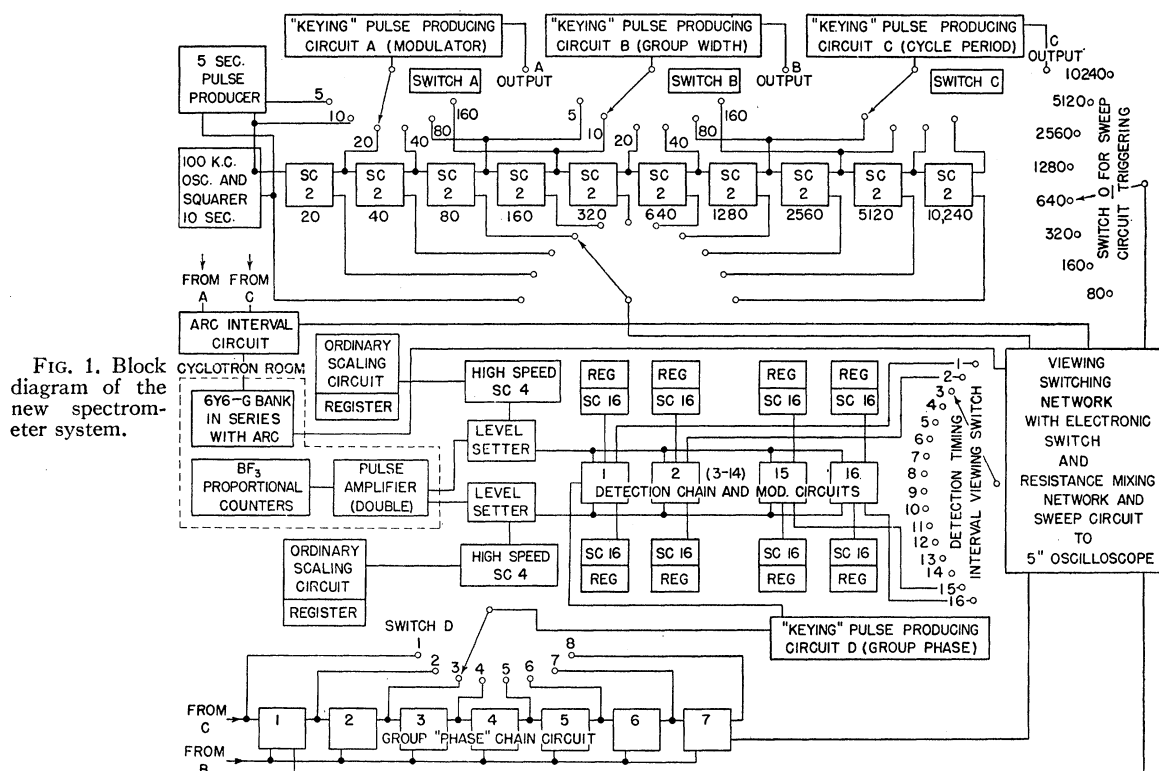


FIG. 1. Block diagram of the new spectrometer system.

resonances by "resonance detector" measurements have given widely different results varying from a resonant energy of less than a volt to about 20 ev. The present measurements show that the Mn cross section for energies below about 30 ev can be well matched by the usual  $1/v$  slope plus a constant term as with boron and lithium. A strong resonance is found near 300 ev and the shape of the transmission curve on the high energy side of this resonance level suggests that another level (or levels) at still higher energies may be present.

### Iridium

The results of the measurements for iridium are presented here since they display more detail than those for any other element yet investigated.

## NEW SPECTROMETER SYSTEM

### Timing Circuits

The block diagram of the new spectrometer system shown in Fig. 1 will serve as the basis for the following discussion. The fundamental timing is provided by a 100-Kc crystal controlled oscil-

lator which is accurate to about 0.01 percent. The 10- $\mu$ sec. wave is "squared up" by limiting amplification to give square wave pulses with about 0.1- $\mu$ sec. rise time. This 10- $\mu$ sec. period square wave is then fed to a special high speed scale of 1024 circuit which provides 20-, 40-, 80-, 160-, 320-, 640-, 1280-, 2560-, 5120-, and 10,240- $\mu$ sec. period square waves. Special care has been taken to ensure a rapid switching action to ensure less than 0.1- $\mu$ sec. time lag in the propagation of the switching pulse down the ten-stage chain of scale-of-2 circuits. By mixing normal and inverted 10- $\mu$ sec. period pulses a 5- $\mu$ sec. period pulse is obtained. Thus accurately synchronized timing pulses with periods ranging from 5  $\mu$ sec. to 10,240  $\mu$ sec. increasing by powers of 2 are available.

In normal operation time of flight measurements of less than 640  $\mu$ sec. (at 6.2 meters) are obtained by using a 1280- $\mu$ sec. period for the complete operation cycle and using thick Cd in the beam to remove all neutrons having times of flight greater than about 800  $\mu$ sec. This prevents overlap from previous cycles.

For time of flight measurements of less than 1280  $\mu\text{sec.}$  (6.2 meters) an operating cycle period of 5120  $\mu\text{sec.}$  is used. Thin Hg filters are used to reduce the intensity of neutrons overlapping from the previous cycle to less than one percent of the main intensity without greatly decreasing the intensity of neutrons of the energies being studied.<sup>2</sup>

For time of flight measurements of 1280 to 5120  $\mu\text{sec.}$  an operating cycle period of 5120  $\mu\text{sec.}$  is also used but the Hg filter is omitted. The increased intensity in this region due to the thermal peak<sup>1</sup> gives the proper ratio of main intensity to overlap intensity. For timings greater than 5120  $\mu\text{sec.}$  a period of 10,240  $\mu\text{sec.}$  is used.

The choice of the length of the operating cycle repetition period is obtained by switch *C* in Fig. 1 which selects the square wave pulse of the desired period. A keying circuit then gives a single sharp pulse at the beginning of each cycle of the square wave. This keying pulse activates other circuits to determine the start of the operating cycle and the start of the cyclotron arc pulse (cyclotron "on time" pulse).

For the method of operation which has been adopted, the cyclotron arc pulse width is always made equal to the detection pulse width since this is most convenient and also gives the maximum intensity for a given over-all resolution width. The usual "on time" (to be denoted  $\tau$ ) is  $\tau = 5, 10, \text{ or } 20 \mu\text{sec.}$  when  $T$  (the operating cycle period) = 1280  $\mu\text{sec.}$  When  $T = 5120 \mu\text{sec.}$  and  $t$  (the neutron time of flight selected by the detection interval) is less than 1280  $\mu\text{sec.}$ , the width  $\tau = 20, 40, \text{ or } 80 \mu\text{sec.}$  is usually chosen. For larger timings,  $t$ , the value of  $\tau = 20, 40, 80, \text{ or } 160$  is chosen. The width of the cyclotron arc and the detection "on time,"  $\tau$ , is selected by switch *A*. The signal obtained is then converted to a single sharp "keying pulse" at the beginning of each cycle of the chosen square wave period to activate the other circuits.

In the new spectrometer system 16 detection intervals are measured simultaneously. These are automatically made adjacent (the spacing between adjacent intervals is equal to the width of each detection interval) and of equal width such that a *group* of 16 adjacent timing intervals is measured simultaneously. The factors involved in the operation may, at this point, best be illus-

trated by an example. Suppose that measurements with high resolution at the high energy end of the spectrum are being made; switch *C* is placed at 1280  $\mu\text{sec.}$  (for  $T$ ) and switch *A* is set at 5  $\mu\text{sec.}$  (for  $\tau$ ). The arc pulse is turned on at the beginning of the cycle by the pulse from *C* and is turned off by the next pulse from *A* so that it is "on" from  $t = 0$  to  $t = 5 \mu\text{sec.}$  This is accomplished by using one stage of a "chain" type scaling circuit to be described below.

The first detection interval (for the *first group*) now extends from  $t = 0$  to  $t = 5 \mu\text{sec.}$ , the second from  $t = 5$  to  $t = 10 \mu\text{sec.}$ , and so on with the 16th detection interval from  $t = 75$  to  $t = 80 \mu\text{sec.}$  Each detection interval circuit is then inactive until the corresponding interval in the next operating cycle.

In order to extend the timing to values greater than 80  $\mu\text{sec.}$ , the whole group of detection intervals is shifted by 80  $\mu\text{sec.}$  to give the *second group* of detection intervals. In practice this is done by simply setting switch *D* to the second position (the details of the operation will be explained below). The first detection interval now extends from  $t = 80$  to  $t = 85 \mu\text{sec.}$  and the 16th from  $t = 155$  to  $t = 160 \mu\text{sec.}$  For still larger timings switch *D* is set at its third position (*third group*) to obtain timings between 160 and 235  $\mu\text{sec.}$

The timing corresponding to each detection interval is expressed as a definite value equal to the time from the beginning of the cycle to the beginning of the detection interval. This also corresponds to the timing between the *center* of the arc pulse interval and the *center* of the given detection interval. This, when later corrected for the over-all time lag of the system (discussed below), specifies the corrected timing being measured. The superimposed resolution width then has the usual significance.

The complete timing interval is thus studied by measuring successive groups each containing 16 intervals. In the above example for high resolution the *first group* contains 16 detection intervals in the range of  $t = 0$  to  $t = 75 \mu\text{sec.}$  corresponding to neutron energies of 50 electron volts and up. The *second group* contains 16 intervals from  $t = 80$  to  $t = 155 \mu\text{sec.}$  corresponding to neutron energies between 10 ev and 50 ev. The *third group* measures from  $t = 160$  to  $t = 235 \mu\text{sec.}$  corresponding to  $E = 4 \text{ ev}$  to 10 ev. The *fourth group* similarly ex-

tends from  $t=240$  to  $t=315$   $\mu\text{sec.}$  or  $E=2.5$  to 4 ev. There are provisions for measuring 8 *groups* and this has always proved adequate for all measurements. In fact groups 5, 6, 7, and 8 are only rarely used.

The choice of the detection *group width* is obtained by setting switch *B* to the proper position. This is normally chosen to be equal to  $16\tau$  as in the above example. It is possible to choose other values for special purposes, however, and this is frequently done.

The above description explains the operation of the spectrometer timing system from a schematic viewpoint to present a general picture of the operation. A more detailed description may now be given. In order to obtain the different *groups* of detection intervals a group chain circuit with 7 stages in series is used. Each stage consists of a trigger circuit which has two stable conditions which may be called "off" and "on." Each stage is normally "off" during the complete operating cycle until it is triggered "on" by a pulse from *C* (first stage) or by the previous stage in the process of going "off." It then remains "on" until the next pulse arrives from *B* which turns it "off" and the next stage "on." This condition of activation starts when the first stage goes "on" at the start of the operating cycle and moves one step along the chain for each pulse from *B* until the last stage goes "off" after which all stages remain "off" until the start of a new operating cycle. The switch *D* selects either the pulse from *C* or the extinguishing pulse from any of the 7 chain stages to give a choice of any of 8 successively spaced pulses for use to start the detection chain circuits at the appropriate time during the operating cycle.

The detection intervals are provided by a similar "chain" of 16 stages. The first stage is turned "on" by the pulse from *D* and the condition of activation is moved along the chain by pulses from *A* (which determine the width of each detection interval). When the last of the detection stages goes "off," all stages remain inactive until the next pulse from *D* during the next operating cycle.

### Detection

The system is now operated with two parallel independent  $\text{BF}_3$  proportional counter detectors

with separate collimating systems. The new counters have cathodes 10 cm in length, about 5-cm diameter, and are filled to 50-cm pressure with purified  $\text{BF}_3$  enriched in  $\text{B}^{10}$  content for greater efficiency. The proper operating voltage for these counters depends on the amplifier gain and may be varied over 500 volts by varying the amplifier gain. At present a potential of 3700 volts is used. The background rate is regularly measured during each "run" by inserting thick  $\text{B}_4\text{C}$  or  $\text{Cd}$  in the beam but it is usually completely negligible. Some trouble was experienced with H.V. "humidity" pulses for a while but this was remedied by continuously blowing dry air over the counters.

### Amplifier, Pulse Discriminator, and Coincidence Circuits

The twin pulse amplifiers have been rebuilt to give greatly improved high frequency response. The outputs of the amplifiers are sent to the level selectors and switching circuits along coaxial lines terminated in their characteristic impedances. A special multivibrator type level selector circuit is used to give a short resolving time, a minimum time lag, and uniform output pulses. Pulses from the level selector are fed to one side of each of 16 coincidence circuits the other input of which is the particular detection interval pulse. The pulses from the coincidence circuits each go to a separate high speed scale-of-2 circuit and then to a standard scale-of-16 circuit (which is normally operated as a scale-of-4). The output of each of these 32 "scale-of-16" circuits then goes to one of 32 registers which indicate the "timed" counts. These are arranged in banks for easy reading.

The output of each level selector circuit also goes directly to a high speed scale-of-4 circuit and then to a standard scale-of-128 circuit and register to indicate the "total counts" in each "channel."

### Arc Modulation

The arc modulation is accomplished by controlling the accelerating voltage to the cyclotron arc. A bank of 12 type 6Y6-G tubes in series with the arc accelerating voltage circuit controls the arc current which is of the order of 5 amperes instantaneous current. For high resolution work this gives instantaneous deuteron power of 5 to 15

kilowatts on the target. Since an internal probe is used with a normal energy setting of about 8 Mev, this corresponds to an instantaneous deuteron current of about 700 to 2000 microamperes at the Be target. A special viewing circuit has been devised to permit accurate viewing of the arc *current* pulse as opposed to the arc voltage pulse. This has proved useful in adjusting the arc filament heating as well as to monitor arc operation.

### Circuit Monitoring

To view the circuit operation extensive viewing circuits have been provided and circuits to compare several wave forms simultaneously. This is accomplished by the use of mixing circuits and an electronic switch circuit of special design. All of the circuits used in the present system were designed especially for this use and have not been described in the literature. To obtain excellent fractional microsecond response speeds the basic scale-of-2 and chain circuits, for example, employ principally type 6AG7 tubes and use plate load impedances of the order of 140, 500, 1000, 2000, and 3000 ohms. Since good high frequency response requires low impedances and thus high plate currents from all tubes, it was necessary to construct regulated power supplies of large current capacities. Thus regulated voltages of 100 volts at 5 amperes, 250 volts at 2 amperes, and -50 volts (bias) at 400 milliamperes are used for the timing circuits.

### GENERAL REMARKS ON THE EXPERIMENTAL RESULTS

#### Resolution Width and Over-All Delay Time

Since the cyclotron arc pulse width and the detection interval widths are equal, the resolution function would be triangular in shape and of width  $2\tau$  if only these factors were involved. For energies above about 0.2 ev the other possible sources of resolution broadening are caused by the counter length, by any extra time smear of the slow neutron pulse leaving the paraffin "source slab," and by effects due to the lack of perfect sharpness of the pulses from the  $\text{BF}_3$  counter-amplifier-level selector system. In addition there will be an over-all delay time correction due to cumulative time lags in the system such as the time for the deuterons to be accelerated

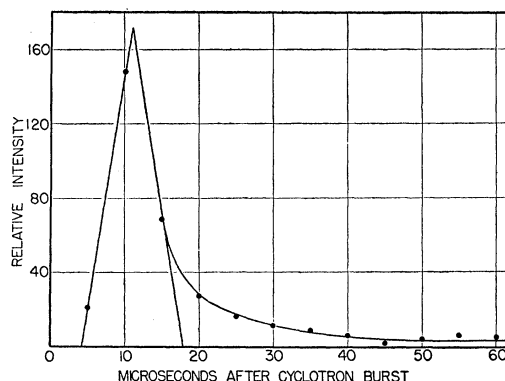


FIG. 2. Experimental resolution curve showing the over-all measured time delay in the system to be 11  $\mu\text{sec}$ .

in the cyclotron (a low energy setting of the Be probe target decreases this effect), for the neutrons to be slowed in the paraffin slab, and the timing between the time when a neutron is captured in the  $\text{BF}_3$  counter and the time corresponding to the center of the resultant pulse from the level selector circuit.

All of the above effects were important in the previous system and are described in the first two references. The net magnitude of these effects was experimentally determined with fair accuracy by placing the detector in a  $\text{B}_4\text{C}$  shield near the source. The intensity *vs.* timing was measured using 5  $\mu\text{sec}$ . "on times" as shown in Fig. 2. This shows that the over-all time lag of the system is now about 11  $\mu\text{sec}$ . The resolution function in this case is roughly triangular in shape and about 10  $\mu\text{sec}$ . ( $2\tau$ ) wide. The "tail" shown on the right of the triangle (Fig. 2) is largely due to the effects of fast neutrons scattered around the cyclotron enclosure. Since the detector is normally outside the water barrier and better source shielding is employed, the magnitude of the "tail" in Fig. 2 is much greater than would be expected for normal operation.

The effect of the 10-cm counter length is to give an uncertainty of  $\pm 5$  cm in the total path length of 620 cm. This gives an extra broadening of the resolution width on a time of flight basis equal to 1.6 percent of the timing involved. This is usually much smaller than the value of  $\tau$  selected. Although the resulting resolution function is no longer simply triangular in shape, it will be nearly so and has been taken to be of this form for simplicity.

*As a result of the above reasoning it has been decided to omit the resolution function from all curves with the understanding that, almost always, the resolution function may be taken as triangular in shape with a width slightly greater than twice the spacing between adjacent points.* It is unusual for the effective width to be as great as three times the spacing between adjacent points so the above rule will permit easy interpretation of the effect of the resolution width on the shape of the experimental curves.

#### Effect of the Thermal Lag from the Source

For energies below about 0.2 eV the lag in the emission of thermal neutrons from the source must be considered. This is caused by the diffusion time of the thermal neutrons in leaving the source. The present paraffin source slab is slightly thinner than the one previously used so the calculated delay time is now about 30  $\mu$ sec. and this value has been used. This means that 4.5  $\mu$ sec./meter must be deducted from the timings and added to the resolution width for timings greater than about 200  $\mu$ sec./meter. For intermediate timings a graded correction factor is used. For the resolution normally used in the thermal region the width of the resolution triangle is less than three times the spacing between adjacent points.

#### Convention Regarding Cross Section and Energy

To simplify the notation it will be understood that cross sections are always expressed in units of  $\times 10^{-24}$  cm<sup>2</sup>/atom, and the symbol  $E$  will refer to the neutron energy in electron volts. The units will usually not be explicitly stated.

#### Significance of Measured Cross Sections at Resonance

Except in the case of Cd where a detailed analysis of the resonance has been made, it is usual for resonances to occur at several eV energy or higher. For these resonances the transmission curve shows a dip at resonance such that the area under the transmission curve is related to  $\sigma_0 \Gamma^2$ , the strength of the level.<sup>2</sup> When the resolution width is large compared to the level half-width there is thus little relation between the value of  $\sigma_0$  (the true cross section at exact resonance) and

$[-(1/n) \log T_{\min}]$ , the cross section calculated directly from the experimental transmission curve. It is possible to say that  $\sigma_0$  is greater than  $[-(1/n) \log T_{\min}]$  but in many cases the ratio of the two values may be of the order of 10 to 1000 and a comparison may be more misleading than helpful. From experience it has been found that curves plotting the measured cross section of a sample in the region of a resonance *vs.* neutron energy (or  $\log E$ ) while of some interest are easily misinterpreted and such questions as the reality of a resonance dip and significance of the magnitude of the dip can better be judged when a curve showing measured transmission *vs.* time of flight is used. To permit easy determination of the neutron energy a neutron energy scale is also given. Also, since the value of the measured cross section away from a resonance is significant, a cross-section scale is usually indicated at the right of each curve. An additional advantage of this method for measurements in the thermal region is the fact that the  $(1/v)$  capture term in the thermal region shows as a straight line when the transmission on a logarithmic scale is plotted as a function of the timing.

#### The Assignment of Resonance Levels to Particular Isotopes

While it is true that each observed resonance in a sample should be assigned to a particular isotope of the element, there is usually insufficient information available to make this assignment. As a result the policy has been adopted of stating the values of  $\sigma$  and  $\sigma_0$  as if only one isotope were present (in terms of the element as a single material). In cases where the proper isotope assignment can be made, the true cross section per atom may be obtained by dividing the uncorrected value by the fractional concentration of the responsible isotope in the natural element. In special cases where this can be done the values will be given in the usual manner first and then special mention will be made of the corrected values.

#### Calculation of $\sigma_0 \Gamma^2$ , the "Strength" of the Level

If  $\sigma_0$  is the cross section at exact resonance for a sample and  $n$  is the number of absorbing atoms

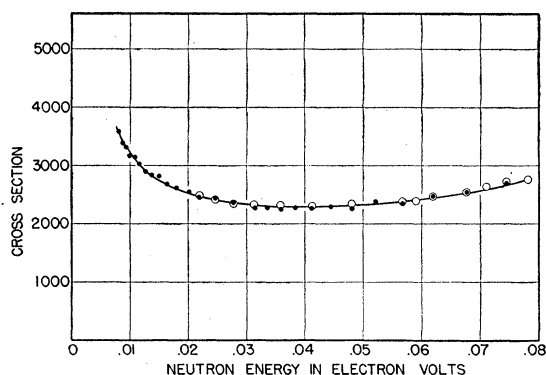


FIG. 3. The slow neutron cross section of cadmium in the energy interval 0-0.08 eV.

● Experimental points for the 43.8 mg/cm<sup>2</sup> sample  
○ Experimental points for the 219 mg/cm<sup>2</sup> sample

The solid line is a theoretical curve using the Breit-Wigner one-level formula with  $E_0=0.176$  eV,  $\Gamma=0.115$  eV, and  $\sigma_0=7200$ .

per square centimeter, then  $T=e^{-n\sigma_0}$  is the true transmission for exact resonance. If  $n\sigma_0$  is large compared with unity it has been shown<sup>2</sup> that the area *above* the transmission *vs.* time-of-flight curve is a function of  $n\sigma_0\Gamma^2$  and, for dips with small area, is proportional to  $(n\sigma_0\Gamma^2)^{1/2}$ . The theory has been developed to permit  $\sigma_0\Gamma^2$  to be determined for such a resonance dip and it has been applied to the cases of In, Ag, Au, and Sb<sup>2</sup> where it probably applies.

From the results of measurements using a number of other elements, however, it has been found that many of the resonance dips are quite small even when rather thick samples are used. After these results were examined there was some question as to whether it was proper to assume that  $n\sigma_0 \gg 1$  for all of these levels. If  $n\sigma_0 \ll 1$  and the level dip area is obtained by a comparatively large level width  $\Gamma$ , the area *above the transmission curve* will be proportional to  $n\sigma_0\Gamma$  rather than to  $(n\sigma_0\Gamma^2)^{1/2}$  while intermediate conditions will apply when  $n\sigma_0$  is neither large nor small. This uncertainty in many cases has tended to discourage the calculation of  $\sigma_0\Gamma^2$  by the usual method. In that case the information presented about a level would be limited to a statement of the position of the level plus what rough evidence can be obtained concerning the relative strength of the level from the appearance of the transmission curve.

After some consideration it has been decided

that a statement of the calculated value of  $\sigma_0\Gamma^2$  should be given but with the understanding that the assumption  $n\sigma_0 \gg 1$  is involved. Since this assumption may sometimes be incorrect it should be understood that the values given are valid only to the extent that this condition is satisfied. Values of  $\sigma_0\Gamma^2$  will always be expressed in units of  $\times 10^{-24}$  (eV)<sup>2</sup> cm<sup>2</sup>/atom, although for simplicity the units will not be explicitly stated.

There is also the possibility that some of the observed resonance dips may be caused by many unresolved levels. In this case the interpretation will be of limited significance. In particular if  $\sigma_0 \gg 1$  for each level and  $\Gamma$  much less than the spacing between levels, the area is proportional to the sum of the  $(n\sigma_0\Gamma^2)^{1/2}$  terms while if  $\sigma_0 \ll 1$  for each level and  $\Gamma$  much less than the spacing between levels, the area is proportional to the sum of the  $n\sigma_0\Gamma$  terms. In particular the "broad" resonances may always be caused by two or more unresolved sharp levels.

## RESULTS

### Cadmium

The samples used for the cadmium transmission measurements were cut from sheets rolled to 0.010" and 0.022" thicknesses. A spectrographic analysis of the cadmium showed less than 0.05 percent of Pb and Tl; less than 0.005 percent of Al, Ag, and Cu; traces of Ca, Cr, Fe, Sn. For all

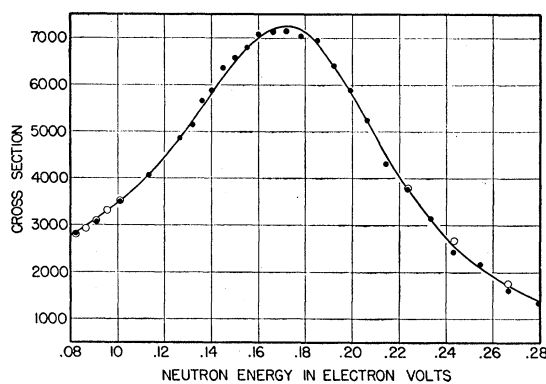


FIG. 4. The slow neutron cross section of cadmium in the energy interval from 0.08 eV to 0.28 eV.

● Experimental points for the 43.8 mg/cm<sup>2</sup> sample  
○ Experimental points for the 219 mg/cm<sup>2</sup> sample

The solid line is a theoretical curve using the Breit-Wigner one-level formula with  $E_0=0.176$  eV,  $\Gamma=0.115$  eV, and  $\sigma_0=7200$ .



the other metals the prominent lines were not apparent, therefore the impurity was probably less than 0.05 percent for arc insensitive elements or less than  $10^{-5}$  percent for arc sensitive elements.

The results of the measurements of the slow neutron cross section *vs.* energy for cadmium are shown in Figs. 3-5. In order to obtain a detailed comparison of the experimental results and the Breit-Wigner one-level formula, it was necessary to use four different sample thicknesses since changes in the total cross section of a factor greater than 1000 were studied. The samples were rolled Cd foil with thicknesses of 43.8 mg/cm<sup>2</sup>, 219 mg/cm<sup>2</sup>, 4.47 g/cm<sup>2</sup>, and 11.03 g/cm<sup>2</sup>. The thick sample was also used to investigate the possibility of other resonances at higher energies as shown in Fig. 6.

The agreement between the theoretical curve and the experimental results in Figs. 3-5 are seen

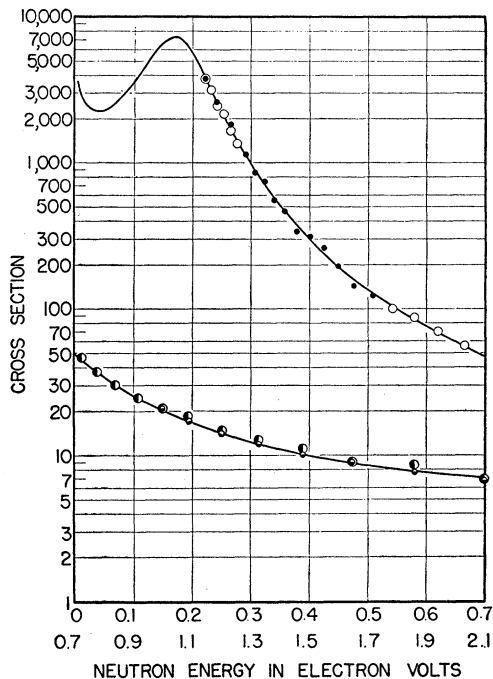


FIG. 5. The slow neutron cross section of cadmium in the energy interval from 0.2 eV to 2.1 eV.

- Experimental points for 43.8 mg/cm<sup>2</sup> sample
- Experimental points for 219 mg/cm<sup>2</sup> sample
- Experimental points for 4.47 g/cm<sup>2</sup> sample
- Experimental points for 11.03 g/cm<sup>2</sup> sample

The solid line is a theoretical curve using the Breit-Wigner one-level formula with  $E_0=0.176$  eV,  $\Gamma=0.115$  eV, and  $\sigma_0=7200$ . A "constant term" of 5.3 has been added to the theoretical curve to account for the scattering cross section.

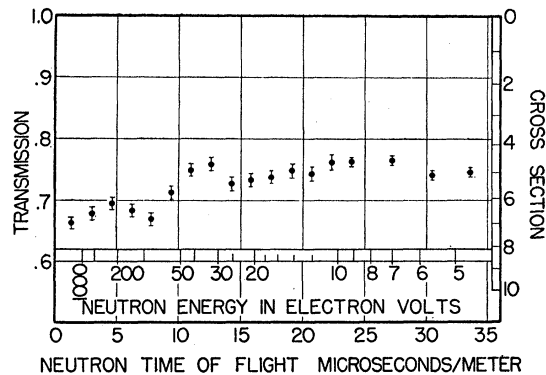


FIG. 6. The slow neutron transmission of 11.03 g/cm<sup>2</sup> cadmium. This curve indicates that the Cd cross section remains approximately constant in the high energy region, although weak levels may be present above 10 eV.

to be within the experimental accuracy of the measurements over the entire region investigated. The statistical uncertainties of the points have not been indicated as their magnitude is often equal in size to the circles used to indicate the experimental points. Individual transmission measurements have a statistical accuracy of the order of (1-3) percent. The degree to which the points fall on a smooth curve illustrates the statistical accuracy involved. Since the best "experimental" curve through the points coincides with the theoretical curve over an extremely wide range of energy and cross section, it is concluded that the Breit-Wigner one-level formula applies for the cadmium resonance over the region investigated.

The sensitivity of the agreement to the choice of the parameters  $E_0=0.176$  eV,  $\Gamma=0.115$  eV,  $\sigma_0=7200$  is such that, if  $\sigma_0$  is held constant a change of  $\pm 0.001$  eV in  $E_0$  or  $\Gamma$  produces a noticeably poorer agreement between the curve and the experimental points. If  $\sigma_0$  is changed by  $\pm 200$  and  $\Gamma$  is adjusted for best fit, the agreement cannot be made to extend over the entire region represented by Fig. 3. The cross section values indicated by the curve in Fig. 5 are not the Breit-Wigner values directly but have been increased by an amount equal to the scattering cross section (constant term) which was chosen to be 5.30. As shown in Fig. 6, the cross section does not reach and remain constant at this value for still higher energies but fluctuates somewhat possibly due partly to experimental uncertainties and perhaps also due to the presence of other

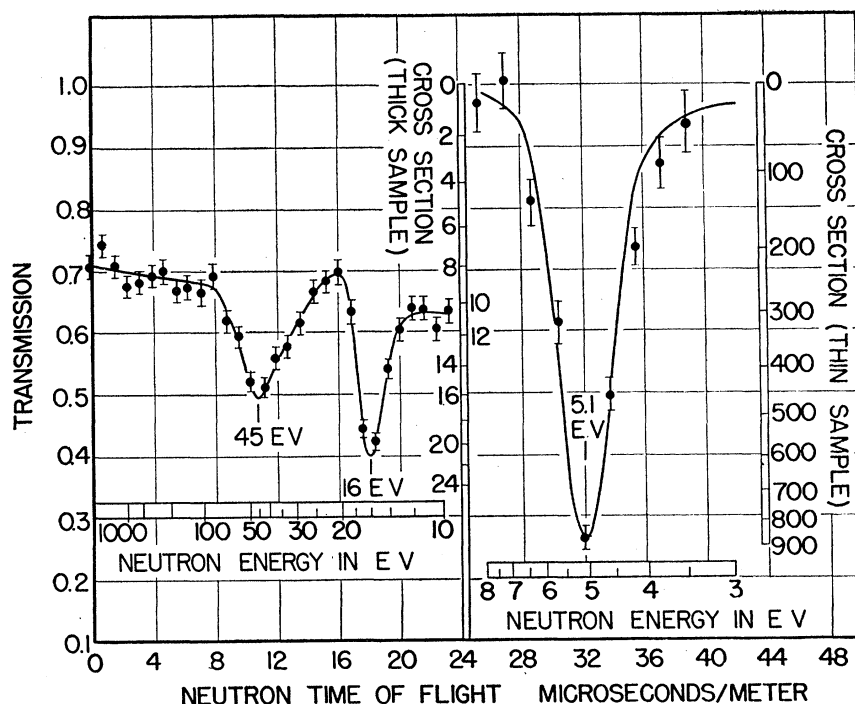


FIG. 7. The slow neutron transmission of silver. The curve on the left shows the transmission of a  $7.84 \text{ g/cm}^2$  sample in the high energy region showing the resonances at 45 eV and 18 eV. The curve on the right shows the transmission of a  $0.276 \text{ g/cm}^2$  sample in the vicinity of the level at 5.1 eV.

weak levels at higher energies. Thus, for example, one or more weak levels may be present near 100 eV. These levels will have a negligible effect on the total cross section in the region covered by Figs. 3-5 so the value  $\sigma_{\text{const}} = (5.30 \pm 0.7)$  is justified below 2 eV. If the cross section in the resonance region also contains a much smaller resonance term for the scattering cross section, this will be included in the main parameters given above. In conclusion, when all possible sources of error are considered, the results for the cadmium parameters have been chosen as

$$\begin{aligned} E_0 &= (0.176 \pm 0.002) \text{ eV}, \\ \Gamma &= (0.115 \pm 0.002) \text{ eV}, \\ \sigma_0 &= (7200 \pm 200) \text{ cm}^2, \\ \sigma_{\text{scatt}} &= (5.30 \pm 0.7) \text{ cm}^2. \end{aligned}$$

The resonance has now been shown<sup>6</sup> to be attributed to  $\text{Cd}^{113}$ , so the isotopic value of  $\sigma_0$  will be 58,500.

<sup>6</sup> B. J. Mayer, B. Peters, and E. H. Schmidt, Phys. Rev. 69, 666 (1946).

### Silver

The samples used for the transmission measurements were of metallic silver. A spectrographic analysis of the silver showed less than 0.05 percent of Cu, Pb; less than 0.005 percent of Mg, Mn, Fe, Tl, and Bi. For all the other metals the prominent lines were not apparent, therefore the impurity was probably less than 0.05 percent for arc insensitive materials or less than  $10^{-5}$  percent for arc sensitive materials.

Since the slow neutron transmission of silver has already been investigated using the earlier form of the spectrometer system,<sup>2</sup> the purpose of the present measurements was to investigate the higher energy region with better resolution. The results of these measurements are shown in Fig. 7. The solid curve shown for the 5.1-eV resonance is a calculated curve based on the parameters given in the previous paper.<sup>2</sup> The agreement is seen to be within the experimental accuracy.

The results of the measurements using the thick sample clearly show the presence of a broad

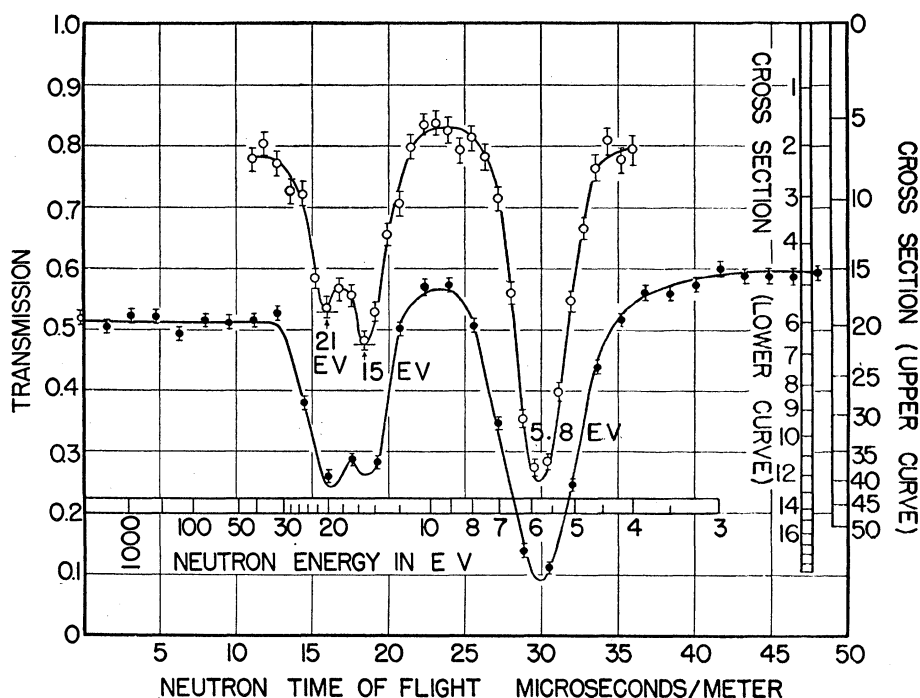


FIG. 8. The slow neutron transmission of antimony. The upper curve shows the transmission of a 6.84-g/cm<sup>2</sup> sample of antimony with 1.8  $\mu$ sec./meter resolution width. The lower curve shows the transmission of a 22.4-g/cm<sup>2</sup> sample of antimony with a 3.6  $\mu$ sec./meter resolution width. The use of a thinner sample and higher resolution permits a partial resolution of the levels at 15 and 21 ev.

level at  $(45 \pm 4)$  ev and a level at  $(16 \pm 1)$  ev in good agreement with the previous results of 13.7 ev and 43 ev. There are three well-established activities with half-lives of 2.3 min., 22 sec., and 225 days induced in silver by  $(n-\gamma)$  reactions.<sup>7,8</sup>

As mentioned above, the measured values of the cross section  $\sigma_{\max}$  at exact resonance has no simple relation to the true value of  $\sigma_0$  for the level since  $\sigma_0$  is usually very much larger than  $\sigma_{\max}$ . The cross section scales are shown only for orientation purposes and are significant only on either side of the resonance dips where the transmission is a slowly varying function of the energy. Thus  $\sigma = (8 \text{ to } 9)$  for  $E = (80 \text{ to } 1000)$  ev as seen in Fig. 7.

In the previous studies<sup>2</sup> the cross section in the thermal region was found to be given by  $\sigma_{\text{thermal}} = [(6.6 \pm 0.5) + (9.05 \pm 0.10)E^{-1}]$ . The

value of  $\sigma_0\Gamma^2$  for the main resonance at 5.1 ev agrees well with the previous value of  $(300 \pm 50)$ . Approximate calculations indicate that  $\sigma_0\Gamma^2 = 24$  and 700 for the levels at 16 ev and 45 ev, respectively. These values are perhaps significant to within a factor of two. Because of the width of the level at 45 ev (as indicated by the fact that the observed width of the dip is several times the resolution width for a small amplitude of dip in the transmission curve), there is reason to suspect that  $\sigma_0\Gamma^2 \ll 1$  rather than  $\gg 1$  as assumed. In this case an approximate calculation indicates that  $\sigma_0\Gamma = 200$  roughly. Also, if the resonance is assumed to be almost resolved in Fig. 7, direct observation indicates that  $\sigma_0 \sim 6$  to 10 and  $\Gamma \sim 25$  ev which gives about a factor of 7 difference for the two assumptions of  $n\sigma_0 \gg 1$  or  $\ll 1$ . If several narrow unresolved levels are responsible the above discussion is meaningless. Since silver has only two almost equally abundant stable isotopes, the true values of  $\sigma_0\Gamma^2$  will be about double the uncorrected values given above for the normal element.

<sup>7</sup> E. Amaldi, O. D'Agostino, E. Fermi, B. Pontecorve, F. Rasetti, and E. Segrè, Proc. Roy. Soc., London A149, 522 (1935).

<sup>8</sup> J. J. Livingood and G. Seaborg, Phys. Rev. 54, 88 (1938); K. Alexeeva, Comptes rendus, U.S.S.R. 18, 533 (1938); A. C. G. Mitchell, Phys. Rev. 53, 269 (1938).

### Antimony

The samples used for the transmission measurements on antimony were cast disks of the metal. A spectrographic analysis of the antimony showed less than 0.05 percent of Ca, Ag, and Si; less than 0.005 percent of Mg, Ni, Cu, and Ge; traces of Co, Pb, and As. For all other metals the prominent lines were not apparent therefore the impurity was probably less than 0.05 percent for arc insensitive materials or less than  $10^{-5}$  percent for arc sensitive materials.

Antimony has also been studied previously using the "old" system.<sup>2</sup> The measurements have been repeated using the "new" system to determine more precisely the position of the resonances and as a comparison of measurements using the two systems. The new results are shown in Fig. 8. The measurements were first made using the 22.4 g/cm<sup>2</sup> sample as shown in the lower curve. The two main resonances are observed as before but the upper level now appears to be composed of two unresolved levels near 15 and 20 ev, respectively. The first level is at  $(5.8 \pm 0.15)$  ev. There is no indication of still higher levels which were previously suspected to exist.<sup>2</sup>

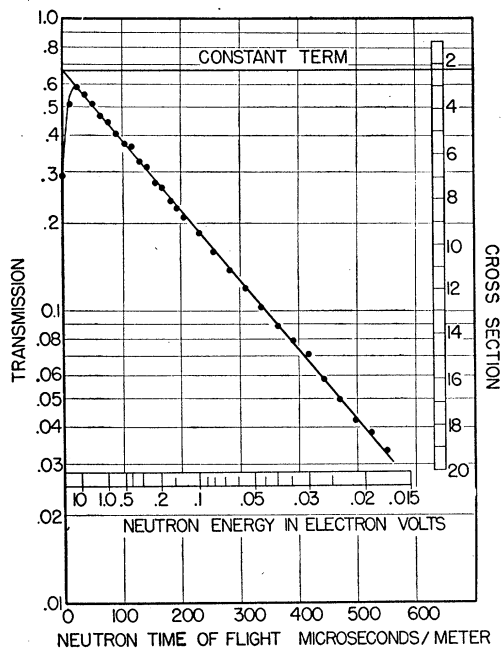


FIG. 9. The slow neutron transmission of 16.24 g/cm<sup>2</sup> of manganese. This curve shows the  $1/v$  type cross section for manganese in the thermal region with  $\sigma = (2.26 + 2.24E^{-1})$  and also shows indications of resonances at higher energies.

In order to investigate the nature of the upper "double" resonance, the measurements were repeated using a 6.84 g/cm<sup>2</sup> sample and double the resolution. The results are shown in the upper curve which more nearly resolves the two peaks. They are seen to be at  $(15 \pm 1)$  and  $(21 \pm 1.5)$  ev. The samples used are the same as were used for the earlier measurements.<sup>2</sup> As previously remarked, the value of  $\sigma_{\max}$ , the "measured" cross section at resonance, is not even approximately equal to the  $\sigma_0$  the true cross section at resonance. There are two well-established activities of 2.8 d. and 60 d. known to be induced in antimony by  $(n-\gamma)$  reactions.<sup>7,9</sup>

In the previous studies<sup>2</sup> the cross section in the thermal region was found to be given by  $\sigma_{\text{thermal}} = [(4.2 \pm 0.5) + (0.64 \pm 0.04)E^{-1}]$ . On the basis of Fig. 8 approximate calculations have been made to determine the values of  $\sigma_0 \Gamma^2$  for each of the three levels assuming that the values are approximately equal for the levels at 15 ev

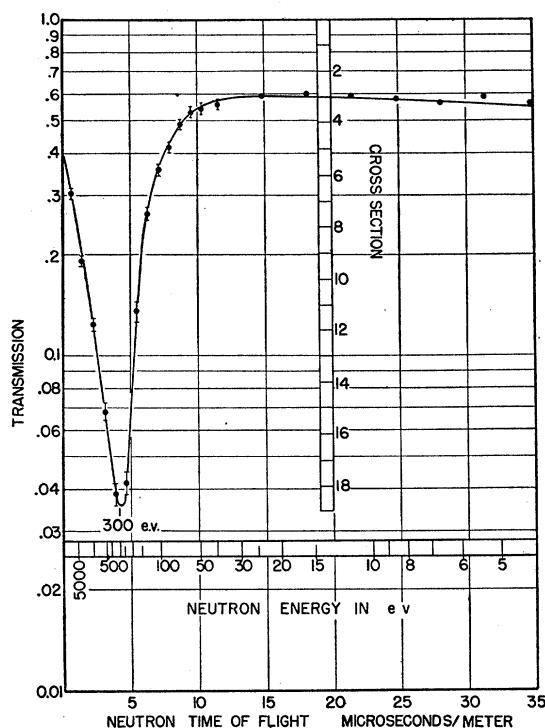


FIG. 10. The slow neutron transmission of 16.24 g/cm<sup>2</sup> of manganese. This curve shows the transmission of manganese in the higher energy region. The position of the resonance level is approximately 300 ev.

<sup>9</sup> J. J. Livingood and G. Seaborg, Phys. Rev. 55, 414 (1939).

and 21 ev. The results which are perhaps significant to within a factor of two, are  $\sigma_0\Gamma^2 = 12, 35$ , and 35 for the levels at 5.8 ev, 15 ev, and 21 ev. Antimony also has only two stable isotopes of almost equal abundance so the above values of  $\sigma_0\Gamma^2$  will be twice as large on an isotopic basis.

It is interesting to note that the cross section above 40 ev is quite constant but *not* equal to the value predicted from the intercept of the thermal  $1/v$  curve.

### Manganese

The results of the measurements using a 16.24 g/cm<sup>2</sup> sample of pure electrolytic manganese are shown in Figs. 9 and 10. It is seen that the cross section below about 30 ev is well matched by the simple  $1/v$  line  $\sigma = [2.26 + 2.24E^{-1/2}]$ . Figure 10 shows that there are no observable resonance levels below the main resonance at  $(300 \pm 40)$  ev. The level is of particular interest since it represents a strong level which has been measured with good resolution in the region of several hundred volts and also since this value is of the order of ten or more times as large as previously reported values for the manganese resonance.<sup>3-5</sup>

Previous determinations of the energy of the manganese resonance have been made using Mn detectors and the boron absorption method to determine the energy. The values reported were 15 ev<sup>3,4</sup> and 37 ev<sup>5</sup> and it is of interest to observe the degree to which such measurements can be in error. The reason for the low values is easily understood by reference to Figs. 9 and 10. Since the Mn resonance occurs so high it was necessary to use a comparatively thick Mn detector for the measurements to obtain sufficient sensitivity whereas an extremely thin sample is required to obtain correct results. When a thin detector is used it is assumed that the absorption can be considered as the sum of that near exact resonance and that in the " $1/v$  region" for energies considerably lower than the resonance energy. In particular it is usually assumed that essentially all of the  $1/v$  absorption is for neutrons having energies below about 0.5 ev which are removed by thick Cd. Whereas this latter condition applies for resonances at a few ev like those of In, Rh, Ag, and Au; the  $1/v$  region in Figs. 9 and 10 is seen to contain a large "area of absorption" (since actual *transmission* of the sample is shown)

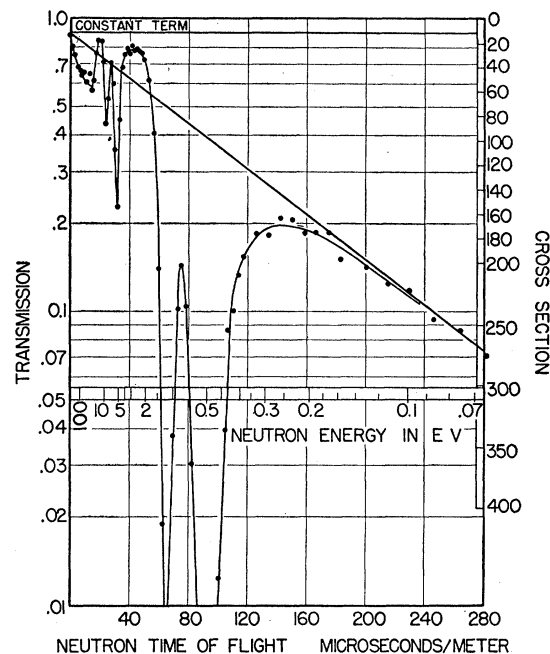


FIG. 11. The slow neutron transmission of 3.08 g/cm<sup>2</sup> of iridium. The curve illustrates the fact that the iridium cross section approaches the  $1/v$  line in the thermal region with  $\sigma = (14 + 64.5E^{-1/2})$  and also shows the several resonance levels in this energy region.

above 0.5 ev. In particular it is probable that over half of the total absorption, which was attributed entirely to the resonance region, was due to absorption in the  $1/v$  region. This easily accounts for the low resonance energies observed.

In Fig. 9 the statistical uncertainty of the points has not been indicated since it is of the order of magnitude of the size of the circles used to represent the experimental points. This is also true of the unmarked points in Fig. 10. It will be observed that there is no indication of a resonance below 0.4 ev as was indicated by other investigators (the above discussion is intended as a general criticism of the boron absorption method for determining the energy of resonant levels rather than as a particular criticism of the papers mentioned). When several levels are responsible for a given activity the boron method will also be misleading. For this reason references to the results of the boron absorption method will be omitted for most elements.

The results may be summarized as follows:

$\sigma = [(2.2 \pm 0.4) + (2.24 \pm 0.05)E^{-1/2}]$  below 30 ev;  
there is a strong resonance with  $E_0 = [300 \pm 40]$  ev.

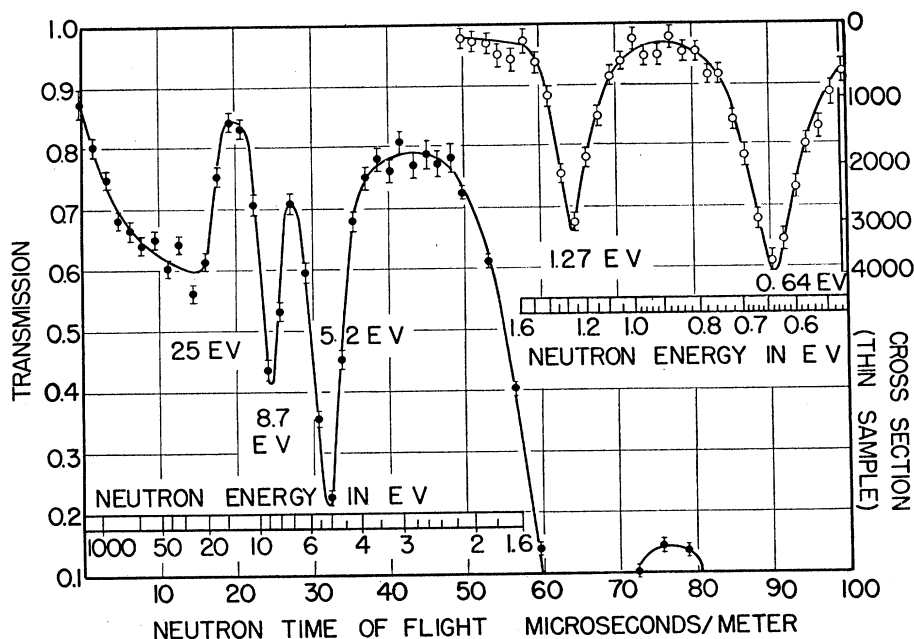


FIG. 12. The slow neutron transmission of iridium. The curve on the left shows the transmission of a 3.08 g/cm<sup>2</sup> sample in the high energy region and shows the levels at 8.7 ev, 5.2 ev, and indications of levels at 25 ev and above. The curve on the right shows the transmission of an 0.0424 g/cm<sup>2</sup> sample which emphasizes the levels at 1.27 and 0.64 ev.

The rise in transmission is slow on the high energy side of resonance indicating that higher (strong) unresolved levels may be present. A value of  $\sigma_0 \Gamma^2$  has not been calculated due to the shape of the curve on the high energy side of the resonance. Since manganese has only one isotope there is no uncertainty in the assignment of the resonance level to this isotope.

### Iridium

The results of the iridium transmission measurements are shown in Figs. 11 and 12. The 3.08 g/cm<sup>2</sup> sample was made from C.P. metallic powder and heated to 800°C in a nitrogen atmosphere. The 0.0424 g/cm<sup>2</sup> sample consisted of the metallic powder mixed in sulphur to obtain uniformity. A spectrographic analysis of the iridium showed that there was less than 0.5 percent of Si; less than 0.05 percent of Ca and Ni; less than 0.005 percent of Mg and Pb; traces of Be, Fe, Rh, Pt, Cu, and Ag. For all other metals the prominent lines were not apparent therefore the impurity was probably less than 0.05 percent for arc insensitive materials and less than 10<sup>-5</sup> percent for arc sensitive materials.

Figure 11 shows part of the data in the thermal region which shows the  $1/v$  slope. Measurements were made up to 480 microseconds/meter and the best straight line for the  $1/v$  slope.  $\sigma = (14 + 64.5E^{-1/2})$  is shown in Fig. 11. The overall features of the transmission curve are shown in Fig. 11 including the resonances near 0.64, 1.27, 5.2, 8.7, and 25 ev.

Iridium has two stable isotopes and there are three known activities of 15 min., 19 hr., and 60 d. induced in Ir by  $(n-\gamma)$  reactions.<sup>7,10</sup>

The resonance region is expanded in Fig. 12 and the results of the measurements at the first two levels using the thin sample are shown. The thin sample was used to obtain more accurate values for the energies of these resonances and to obtain higher values for the lower limits of the  $\sigma_0$  values at exact resonance. It is seen that measured values of  $\sigma_{\max}$  of about 4000 and 3000 were obtained so the  $\sigma_0$  values for the resonances are probably equal to or greater than 5000.

<sup>10</sup> E. McMillan, M. Kamen, and S. Ruben, Phys. Rev. 52, 375 (1937); M. L. Pool, J. M. Cork, and R. L. Thornton, Phys. Rev. 52, 239 (1937); V. Fomin and F. G. Hontesmans, Physik. Zeits. Sowjetunion 9, 273 (1936); R. Jaechel, Zeits. f. Physik 110, 330 (1938).

The results for iridium may be summarized:

1.  $\sigma_{\text{thermal}} = [(14 \pm 6) + (64 \pm 2)E^{-1}]$ .
2. For the first resonance:  
 $E_0(0.64 \pm 0.015)$  ev,  
 $\sigma_0 \Gamma^2 = (5 \text{ to } 20) \times 10^{-24} (\text{ev})^2 \text{ cm}^2/\text{atom}$ ,  
 $\sigma_0 \geq 4500$  (probably).  $\Gamma \leq 0.07$  ev (probably).
3. For the second resonance:  
 $E_0 = (1.27 \pm 0.04)$  ev,  
 $\sigma_0 \Gamma^2 = (5 \text{ to } 20)$ ,  
 $\sigma_0 \geq 4000$  and  $\Gamma \leq 0.07$  ev (probably).
4.  $\sigma = (25 \pm 4)$  for  $2.2 \text{ ev} \leq E \leq 3.5 \text{ ev}$ .
5. For the third resonance  
 $E_0 = (5.2 \pm 0.2)$  ev,  
 $\sigma_0 \Gamma^2 = 55$  roughly.
6. For the fourth resonance:  
 $E_0 = (8.7 \pm 0.3)$  ev,  
 $\sigma_0 \Gamma^2 = 50$  roughly.
7.  $\sigma = (18 \pm 3)$  near  $E = 14$  ev.
8. For the "fifth" resonance  
 $E_0 = (25 \pm 5)$  ev.
9. The shape of the transmission curve for  $E > 25$  ev indicates that probably more levels are present at higher energies so  $\sigma_0 \Gamma^2$  has not been calculated for this "level."

10. Iridium has the isotopes  $\text{Ir}^{191}$  and  $\text{Ir}^{193}$  of 38.5 percent and 61.5 percent abundance, respectively. The above values of  $\sigma_0$  and  $\sigma_0 \Gamma^2$  for the resonances are uncorrected values for the natural element. Depending on which isotope is responsible for a given level, the values should be increased by a factor somewhat greater or somewhat less than two to give the true values for the responsible isotope.

### Conclusion

Since the measurements were made which have been described in two previous papers<sup>1,2</sup> slow neutron transmission *vs.* time of flight measurements have been made for a large number of elements and the slow neutron spectrometer system has been considerably improved. In this first of the new series of papers describing these measurements, the results for Cd, Ag, Sb, Mn, and Ir, have been presented and other results will be presented soon in subsequent papers. This work represents, in all, several thousand hours of cyclotron running time. We wish to thank those who have made this work possible and assisted in the measurements.

## Angular Momentum of Photons

JOSÉ A. BALSEIRO

*Córdoba Observatory, Córdoba, Argentina*

(Received August 12, 1946)

The theory of elementary particles permits one to attribute well-defined angular momentum expressions to a given radiation field. A few simple examples are discussed, which involve systems of two photons, and of one atom and one photon, and which permit one to account for the conservation of total angular momentum. Conservation of total angular momentum, including radiation, is, however, of little practical importance, because spatial orientation of a given system requires, in general, the use of external magnetic fields, which perturb the angular momentum balance.

### 1. INTRODUCTION

ACCORDING to the field theory of elementary particles, angular momentum expressions can be attributed to a given particle field, which, in general, can be divided into an orbital angular momentum and a spin

part.<sup>1</sup> In the particular case of electromagnetic radiation, however, no gauge invariant separation between spin and orbital momentum is possible.<sup>2</sup>

<sup>1</sup> F. J. Belinfante, *Physica* 6, 887 (1939); W. Pauli, *Rev. Mod. Phys.* 13, 203 (1941).

<sup>2</sup> L. Rosenfeld, *Mém. Acad. Roy. Belg. (Cl. Sc.)* 18, 562 (1942).